Agricultural and Forest Meteorology 204 (2015) 1–9

Contents lists available at ScienceDirect

Agricultural and Forest Meteorology

journal homepage: www.elsevier.com/locate/agrformet

Does decadal climate variation influence wheat and maize production in the southeast USA?

Di Tian[a,b,*], Senthold Asseng[a], Christopher J. Martinez[a], Vasubandhu Misra[c], Davide Cammarano[d], Brenda V. Ortiz[e]

[a] Department of Agricultural and Biological Engineering, University of Florida, Gainesville, FL 32611, USA
[b] Department of Civil and Environmental Engineering, Princeton University, Princeton, NJ 08544, USA
[c] Department of Earth, Ocean and Atmospheric Sciences and Center for Ocean-Atmospheric Studies, Florida State University, Tallahassee, FL 32306, USA
[d] James Hutton Institute, Invergowrie, Dundee, DD2 5DA Scotland, UK
[e] Crop, Soil, and Environmental Sciences Department, Auburn University, Auburn, AL 36849, USA

ARTICLE INFO

Article history:
Received 2 September 2014
Received in revised form 15 January 2015
Accepted 20 January 2015

Keywords:
Crop simulation models
Decadal climate variability
Wavelet analysis
Atlantic Multi-decadal Oscillation
Pacific Decadal
Oscillation
North Atlantic Oscillation

ABSTRACT

Linking decadal variability with short-term variability could be potentially exploited for improving seasonal climate forecasting for assisting crop management decisions. The objective of this study was to explore whether there are decadal variations in wheat (winter crop) and maize (summer crop) production and whether these decadal variations correlate with any known variations of climate. Over one hundred years of wheat and maize yields were simulated using process-based crop models with dynamically downscaled daily reanalysis data over four locations in the southeast USA. Using wavelet and cross-wavelet analysis, we found that winter crop yields were dominated by 10- and 22-year decadal oscillations; the decadal variations of winter crop yields were driven by decadal variations of winter temperature and spring precipitation; no decadal variations were detected for summer crop yields and summer precipitation and temperature. Cross-wavelet analysis showed that the decadal variations of winter crop yields were correlated with indices of the annual Atlantic Multi-decadal Oscillation (AMO), the annual Pacific Decadal Oscillation (PDO), and the winter North Atlantic Oscillation (NAO). Therefore, this knowledge of decadal climate variability could potentially be leveraged to predict winter seasonal yields of crops.

© 2015 Elsevier B.V. All rights reserved.

1. Introduction

Climate factors have a major influence on crop production (Hoogenboom, 2000). Variability of climate from one year to another poses risks on decision-making of crop management. For example, higher or lower than normal precipitation (drier or wetter season type) can cause damages or bring benefits to farmers. If these climate conditions can be forecasted in advance, decision-makers can benefit from using this information to change their strategies to adapt to the upcoming season type. For example, a forecast of the season type (e.g., wet or dry) before the start of the season could potentially be used to adjust crop management strategies to save input costs in dry seasons and to increase inputs in wet seasons to get higher achievable yields (Asseng et al., 2012a,b).

Teleconnections refer to statistical associations among different climatic variables among large distances. Recent studies have focused on using the teleconnection of large-scale climate patterns with local climate to improve seasonal crop management (e.g., Bannayan et al., 2010; Brown, 2013; Jarlan et al., 2013; Maxwell et al., 2013; Royce et al., 2011; Vizard and Anderson, 2009). In the southeast USA, agricultural yields have found to be influenced by the El Niño South Oscillation (ENSO) (e.g., Hansen et al., 1998, 1999; Royce et al., 2011), as well as other large-scale climate indices including Pacific/North American teleconnection pattern, tropical North Atlantic and eastern tropical Pacific sea surface temperature (SST), and Bermuda high indices (Martinez et al., 2009; Martinez and Jones, 2011). However, most of these studies were based on correlation or regression approaches that assumed the teleconnection relationships did not change through time, but the variability of large-scale climate patterns are often non-stationary processes (e.g., Coulibaly and Burn, 2004) and their relationships with crop yields may change over time. Besides using observed climate teleconnections, GCM-based seasonal forecast tools have

* Corresponding author at: E312 Engineering Quadrangle, 59 Olden Street, Princeton, NJ, 08544, USA. Tel.: +1 609 258 5334.
E-mail address: dtian@princeton.edu (D. Tian).

http://dx.doi.org/10.1016/j.agrformet.2015.01.013
0168-1923/© 2015 Elsevier B.V. All rights reserved.

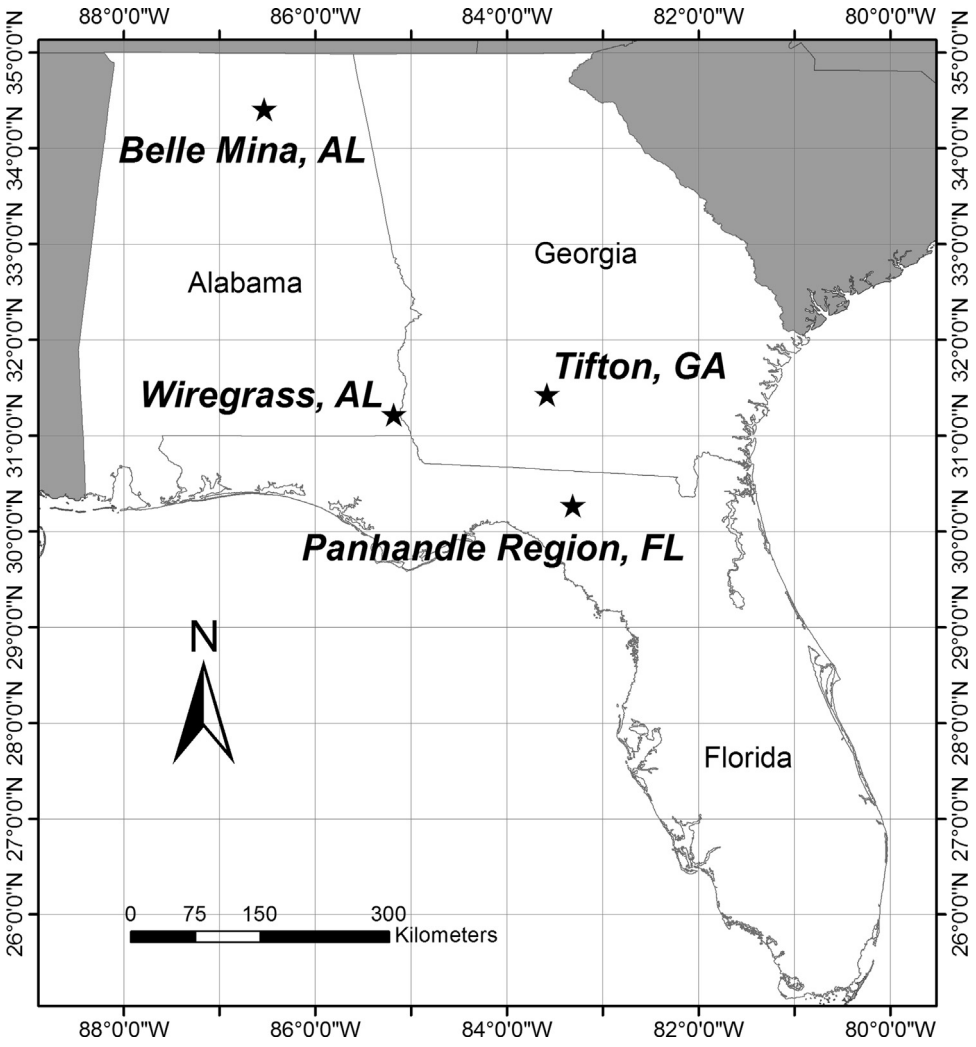

Fig. 1. Study locations in three states of the Southeast USA.

also been used to improve crop management systems in different regions (e.g., Asseng et al., 2012a,b; Baigorria et al., 2010, 2008a,b; Cantelaube and Terres, 2005). However, since the skills of GCMs were still marginal, any crop management improvements from this strategy are limited by the forecast skill of a GCM.

Decadal climate variability information can be potentially combined with the information of short-term climate variability and GCM-based forecasts to further improve seasonal forecasting for crop management. To make use of decadal climate information, the prerequisite step is to know whether there are decadal variations in historical crop production and whether these decadal variations correlate with any known variations of climate. Crop yield and climate data over multiple decades or even a century can be used to investigate the impact of decadal climate on crop yields. Since variation in crop yields is driven by numerous factors not only including fluctuations of climate but also agronomic management (e.g., sowing date, cultivar choice, fertilizer amount, plant density), in this study, dynamic crop simulation models (CSMs) were used as a tool to study the response of crop yields to climate variations by keeping all other factors constant over time. CSMs allow simulating the growth and development of crops beyond a single experimental site, and thus can be used to conduct regional climate impact studies. Climatic inputs such as daily precipitation, temperature, and solar radiation are particularly important for CSMs to simulate crop growth and development (van Ittersum et al., 2003). Since complete sets of these observed weather variables are difficult to obtain over a period of multiple decades at a regional scale, reanalysis data, which provides a temporally and spatially consistent representation of the observed weather, can be used as a surrogate for inputs into CSMs (e.g., Cammarano et al., 2013; Challinor et al., 2005).

This study is aimed to assess the decadal variability of crop yields and the possible links to dominant climatic patterns. Most previous assessment studies were based on correlation- or regression-based analysis between crop yields and the teleconnection pattern indices by assuming stationary time series. However, wavelet analysis has revealed that climatic patterns are non-stationary processes, since their variance, frequency, and duration changes through time (Grinsted et al., 2004; Torrence and Compo, 1998). The time series of climate-driven simulated crop production may also exhibit non-stationarity. Therefore, using wavelet analysis as opposed to traditional stationary approaches can capture the intermittent features of the relationship between time series of simulated crop production and climate factors and can enhance the understanding and potential predictability of crop yields. While in recent years, wavelet analysis has been widely used in detecting non-stationary features and correlations in geophysical time series such as climate and hydrology (e.g., Carey et al., 2013; Liang et al., 2010), this method has not yet been used in assessing the impact of climate variability on crop yields. To the authors' knowledge, this study is the first to introduce wavelet methods to climate impact assessment of crop production.

Wheat (winter crop) and maize (summer crop) are two of the most important crops in the world. The main objectives of this study were to explore possible decadal variations and their drivers for wheat and maize production in the southeast USA using wavelet methods. CSMs driven by reanalysis data were used to simulate trend-free crop production in multi-decadal time scales. Wavelet analysis methods were then applied to analyze the climate driven crop productions and their relationships to climate patterns.

2. Materials and methods

2.1. Reanalysis dataset

Reanalysis data used in this study was from the Florida Climate Institute-Florida State University Land–Atmosphere Reanalysis data set for the southeastern United States at 10-km resolution version 1.0 (FLAReS1.0, http://coaps.fsu.edu/pub/Southeast/FLAReS1.0/daily/) (DiNapoli and Misra, 2012; Misra et al., 2013). DiNapoli and Misra (2012) and Misra et al. (2013) noted that local climate variability and its teleconnections with large-scale climate patterns are well-represented by FLAReS1.0 on seasonal, interannual, and decadal time scales, which made it suitable for local climate impact studies. FLAReS1.0 was dynamically downscaled from the 20th Century Reanalysis (Compo et al., 2011) using the Regional Spectral Model. It archived 106 years of precipitation, solar radiation, mean temperature, and maximum and minimum temperature data in daily time steps from 1903 to 2008. These daily weather variables were used as inputs into CSMs to simulate crop production and allowed for the examination of decadal scale variations of crop production in the southeast USA.

2.2. Crop simulations

Crop simulations were performed using the DSSAT 4.5 (Hoogenboom et al., 2010; Jones et al., 2003) CERES-maize model (Jones et al., 1986) and the APSIM-Nwheat model version 1.55s (Asseng, 2004). The winter wheat cultivar Baldwin and a mid-season maize hybrid were used in this study because these two cultivars are representative for wheat and maize grown in the southeast USA. The models were calibrated and evaluated using trail data from three locations in Alabama for wheat cultivar Baldwin (from 2009 to 2011) [Tennessee Valley Research and Extension Center at Limestone County located in Belle Mina, northern Alabama (34°41′N, 86°53′W), Wiregrass Research and Extension Center at Henry County Headland, southern Alabama (31°22′N, 85°18′W), and E.V. Smith Research and Extension Center at Macon County, Shorter, Central Alabama (32°25′N, 85°53′W)], and Tifton in Georgia (31°71′N, 83°34′W) for a mid-season maize hybrid (from 1997 to 2008). The mid-season maize hybrid was simulated for the mean yield and mean life cycle across a set of about 20 or more maize hybrids for a given season using Tifton, Georgia variety trials. So the maize cultivar used in this study is a composite representative hybrid. The root mean square error (RMSE) for calibration and validation was 1.89 t ha^{-1} for maize and 0.74 t ha^{-1} for wheat. The calibrated genetic coefficients are shown in Table 1.

We assume that the same cultivars are applicable for the region, including northern Florida, Alabama and Georgia. Four representative locations were selected for maize and wheat model simulations (Table 2 and Fig. 1) using the calibrated cultivars (Table 1). An important implication of using the same cultivar across the region is that the findings are due differences in climate as the main subject and not influenced by different cultivars.

A soil with a high water-holding capacity (silty–clay soil) was used for four locations in the southeast USA after Cammarano et al. (2013) because this type of soil is representative for an average soil for the southeast USA. Both maize and wheat models were simulated with a rainfed (non-irrigated) scheme and with no nitrogen (N) stress by switching N limitations off (DSSAT) and supplying plenty of N fertilizer (APSIM-N wheat). The planting density was 6 and 350 plants m^{-2} for maize and wheat, respectively. We initialized the crop models with soil water content at 50% above the lower

Table 2
Study locations and crop management.

Locations	Wheat sowing	Maize sowing	Latitude	Longitude
Belle Mina, AL (N-AL)	15-October	15-April	34.41	−86.53
Wiregrass, AL (S-AL)	29-October	20-March	31.22	−85.18
Tifton, GA (S-GA)	15-November	20-March	31.43	−83.58
Panhandle Region, FL (N-FL)	30-November	20-March	30.27	−83.31

Table 1
Genetic coefficients used to describe a mid-season maize hybrid for DSSAT crop model and the wheat cultivar Baldwin for the N-wheat model (from Cammarano et al., 2013).

Maize genetic parameters							
	P1	P2	P5	G2	G3	PHINT	
	GDD	–	GDD	# per plant	mg d^{-1}	GDD	
Mid-cycle	300	0.3	990	795	8.1	39	
Wheat genetic parameters							
	P1V	P1D	P5	Grno	Fillrate	Stmwt	Phylo
	–	–	GDD	Kernel g^{-1} stem^{-1}	mg kernel^{-1} day^{-1}	g stem^{-1}	GDD
Baldwin	3.1	4.2	750	25.7	2.2	3	123

Maize coefficients
P1: Thermal time from seedling emergence to the end of the juvenile phase (expressed in degree days above a base temperature of 8 °C) during which the plant is not responsive to changes in photoperiod.
P2: Extent to which development (expressed as days) is delayed for each hour increase in photoperiod above the longest photoperiod at which development proceeds at a maximum rate (which is considered to be 12.5 hours).
P5: Thermal time from silking to physiological maturity (expressed in degree days above a base temperature of 8 °C).
G2: Taximum possible number of kernels per plant.
G3: Kernel filling rate during the linear grain filling stage and under optimum conditions (mg day^{-1}).
PHINT: Phylochron interval; the interval in thermal time (degree days) between successive leaf tip appearances.
Wheat coefficients
P1 V: Sensitivity to vernalization.
P1D: Sensitivity to photoperiod.
P5: Thermal time from start of grain filling to maturity.
Grno: Coefficient of kernel number per stem weight at the beginning of grain filling.
Fillrate: Maximum kernel growth rate.
Stmwt: Potential final dry weight of a single stem (excluding grain).
Phylo: Phyllocron interval.

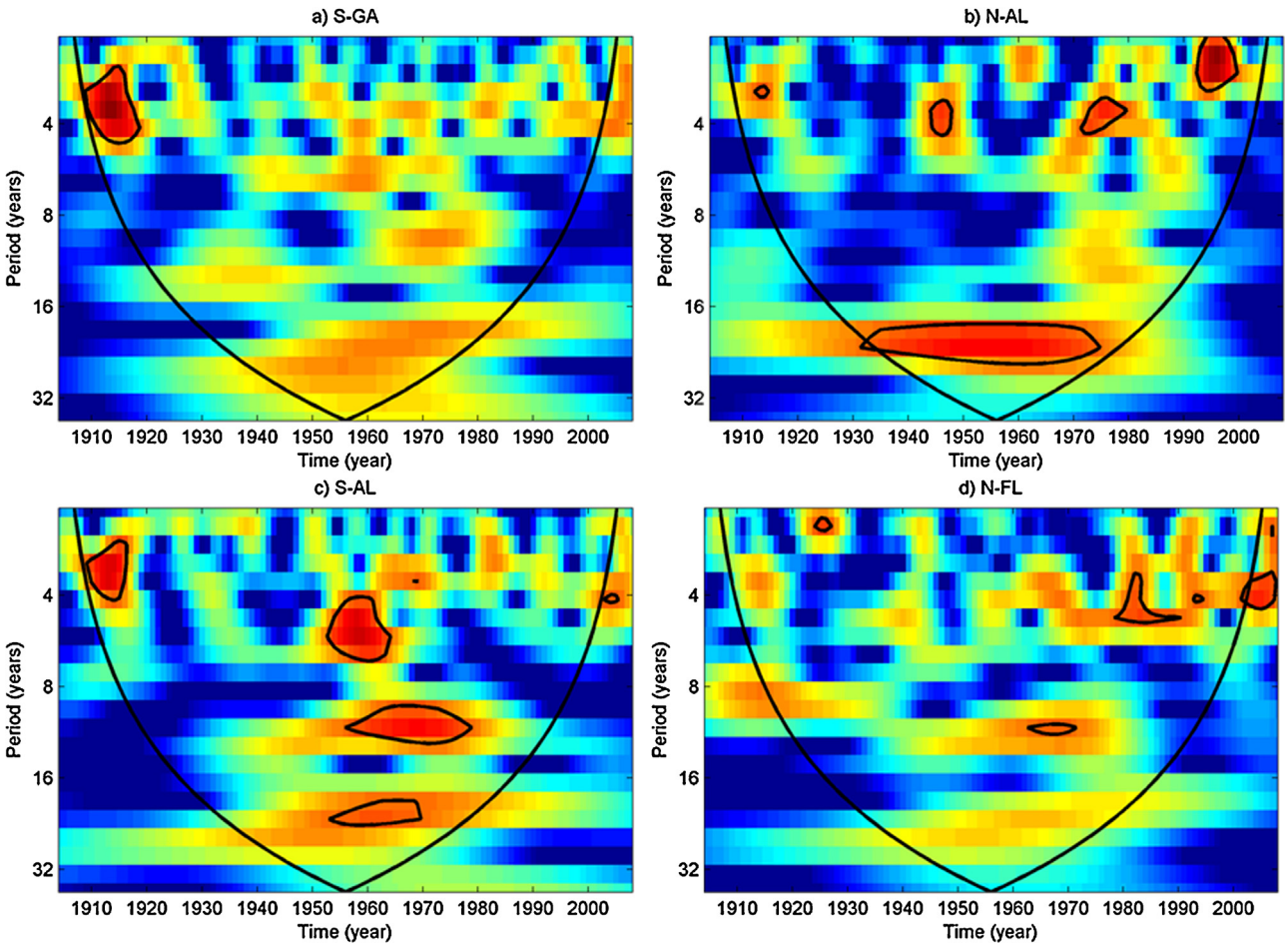

Fig. 2. Wavelet power spectrum for wheat yields from 1903 to 2008 at four locations in the southeast USA: (a) N-AL, (b) S-AL, (c) S-GA, and (d) N-FL. Yellow to orange to red color pixels represent increasing wavelet power spectrum, blue colors show a low wavelet power spectrum. The black contour (surrounding red and orange areas) designates the 5% significance level against "red noise". Inside the black cone shape contour is the region without an edge effect. Outside the black cone contour is the region of cone of influence (COI) – which is due to the finite length of the time series where the edge effects become important and distort the results[For interpretation of the references to color in this figure legend, the reader is referred to the web version of this article].

limit (also called the permanent wilting point) three months before the planting date in order to take account into pre-sowing rainfall. This initial soil water content was reset in the models before planting to avoid any variability in water carry-over effects. Harvest for both crops occurred automatically at maturity. The crop growing seasons were different for maize and wheat at the different locations. The planting dates in these simulations were chosen as average "usual planting dates" (Table 2), which are most "representative" planting dates for these four locations (Cammarano et al., 2013). Following Cammarano et al. (2013), we define the growing season for summer maize from March to July and for winter wheat from October to May. A wheat growing season was across two years (for example when sown in Fall 1979, it was harvested in Spring 1980) and a maize crop was sown and harvested in the same year. Since the wheat growing season was across two years, wheat production was simulated for 105 years, starting from Fall 1903. Maize production was simulated for 106 years, starting from Spring 1903.

2.3. Selected climate indices

This study included three large-scale climate patterns that have shown impacts on the regional climate of the southeast USA. These selected indices were the annual mean Atlantic Multidecadal Oscillation (AMO) index, annual mean Pacific Decadal Oscillation (PDO) index, and winter (December thru March) index of the annual North Atlantic Oscillation (NAO). These indices have been found to be the predominant patterns for displaying variability of decadal timescales and have impacts on the regional climate in the southeast USA (Enfield et al., 2001; McCabe et al., 2004; Seager et al., 2010). The AMO was defined as the leading mode of detrended North Atlantic Ocean Sea Surface Temperatures (SSTs; Enfield et al., 2001) and was obtained from the Physical Sciences Division of the Earth Systems Research Laboratory (http://www.esrl.noaa.gov/psd/data/timeseries/AMO/). The annual mean AMO index was calculated as the average of the unsmoothed monthly AMO index for each year. The PDO was defined as the first principal component of SST anomalies in the North Pacific Ocean (poleward of 20°N) after the global mean SST anomalies has been removed (Mantua et al., 1997). The monthly PDO index was obtained from the Joint Institute for the study of Atmosphere and Ocean at the University of Washington (http://jisao.washington.edu/pdo/PDO.latest). The annual mean PDO index was the average of the monthly PDO index for each year. The winter index of the NAO used in this study was based on the difference of normalized sea level pressure between Lisbon, Portugal and Stykkisholmur/Reykjavik, Iceland and was obtained from the Climate Analysis Section of the National Center for Atmospheric Research (Hurrell and National Center for Atmospheric Research Staff, 2014).

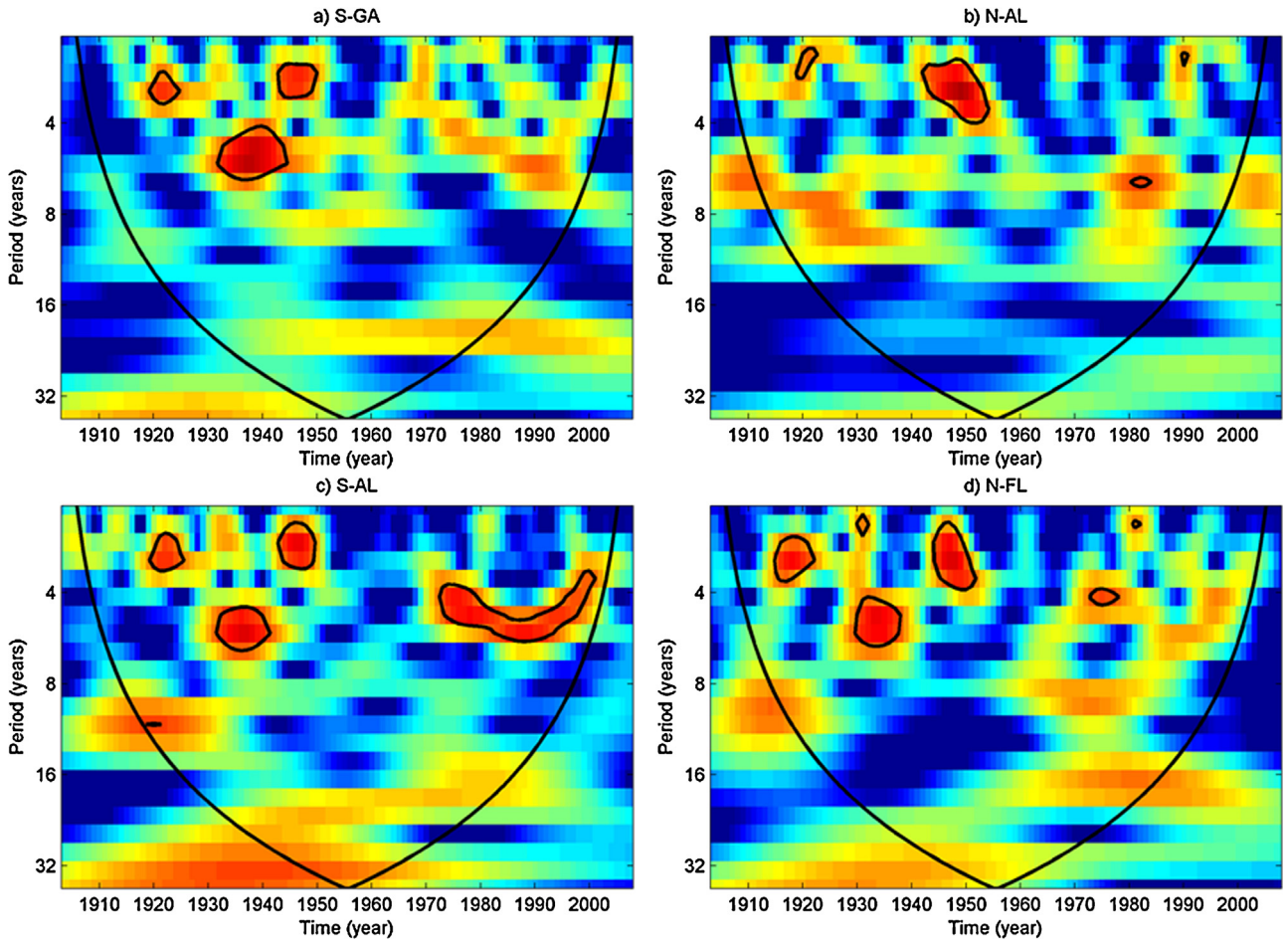

Fig. 3. As in Fig. 2, but for maize yields.

2.4. Wavelet method

The continuous wavelet transformation (CWT) was used to detect intermittent periods of a time series. The cross wavelet transformation (XWT) was applied to detect localized relationships between two time series (weather variables and simulated crop productions, or climate indices and simulated crop productions). The following is a brief summary of CWT and XWT relevant to this study. For a more detailed description of CWT and XWT see Torrence and Compo (1998) and Grinsted et al. (2004). The CWT decomposes a time series from the time domain to the time-frequency (or time-period) domain. The CWT of a discrete sequence x_n is defined as the convolution of x_n with a scaled and translated version of $\psi_o(h)$:

$$W_n(s) = \sum_{n'=0}^{N-1} x_{n'} \psi^* \left[\frac{(n'-n)\delta t}{s} \right] \quad (1)$$

where n is the localized time index, s is the scale, δt is the sampling period, N is the number of points in the time series, and the (*) indicates the complex conjugate. The wavelet power spectrum is defined as $|W_n(s)|^2$. Large wavelet power indicates dominant period. $\psi_o(h)$ is the wavelet function (or mother wavelet). The Morlet wavelet function was used in this research and is written as:

$$\psi_0(\eta) = \pi^{-1/4} e^{i\omega_0 \eta} e^{-\eta^2/2} \quad (2)$$

where η is the nondimensional time factor, ω_o is the nondimensional frequency. The global wavelet spectrum is calculated as:

$$\bar{W}^2(s) = \frac{1}{N} \sum_{n=0}^{N-1} \left| W_n(s) \right|^2 \quad (3)$$

The XWT was used to examine whether regions in time-frequency space with large common power have a consistent phase relationship (Grinsted et al., 2004). The XWT of two time series x_n and y_n is defined as $W^{XY} = W^X W^{Y*}$, where (*) denotes complex conjugate. The cross wavelet power is defined as $|W^{XY}|$. The complex argument $\arg(W^{XY})$ can be interpreted as the local relative phase between x_n and y_n in the time frequency space.

The cone of influence (COI) is the region of the wavelet or cross-wavelet spectrum in which edge effects become important and distort the results. The statistical significance (95%) of the wavelet and cross-wavelet power spectrums was assessed relative to the null hypothesis that the time series was generated as red noise (Torrence and Compo, 1998).

3. Results

3.1. CWT of wheat and maize yields

CWT of simulated annual wheat and maize yields are shown in Figs. 2 and 3, respectively. The wheat yield oscillations were dominated by decadal variability of 10- and 22-year periods and a short-term 4 year variability (i.e., orange to red areas, statistically significant when circled with black line) at four locations (N-AL,

S-AL, S-GA, and N-FL) in the southeast USA. The wavelet power spectrums of wheat yields were high from the 1960s to 1980s for a 10-year period and from the 1930s to 1980s for a 22-year period. It is worthwhile to note that the significance regions around 10 and 22 year periods were different for all 4 sites. N-AL and S-AL had the greatest 5% significance regions around 10 and 22 year periods and showed the strongest occurrence of decadal variations. While N-FL and S-GA had high wavelet power spectrums around 10 and 22 year periods, they had very small or no 5% significance regions compared to the N-AL and S-AL. This difference implicates that the western region had stronger decadal climate variations than in the eastern region of the southeast USA and the strongest decadal climate variations occurred in the northwestern region of this study area and therefore, drove the decadal variations of simulated wheat yields. The maize yield oscillations were dominated by short-term 4-year periods but no decadal variations were found. Fig. 4 is the 11-year and 5-year moving average of the time series of wheat yields after standardization by subtracting the mean and dividing the standard deviation at four locations in the southeast USA. The 22-year period (and 10-year period) oscillations are clearly seen during the 1930–1980s (and the 1960–1980s), which confirms the findings of CWT in Fig. 2.

Fig. 5 is a 11-year and 5-year moving average of the time series of maize yields after standardization by subtracting the mean and dividing the standard deviation at four locations in the southeast USA. 22-year period (and 10-year period) oscillations cannot be seen in this figure. Fig. 5 shows a longer oscillations (more than 30 years) in the early half of the time series. While CWT has identified these longer oscillations, they are within the COI where the wavelet transformations are affected by the edge effect (Fig. 3).

3.2. XWT of crop yields and weather variables

Decadal variations of crop yields can be driven by various weather factors, including daily maximum and minimum air temperatures and precipitation. Since no decadal variations were detected for maize yields, the XWT analysis is only shown for wheat yields. The XWT was firstly applied for wheat yields and mean temperatures or precipitation over the growing season (October–May) at four locations in the southeast USA, but no relationships at decadal scales were detected (not shown). The XWT was then conducted for wheat yields and monthly and seasonal mean temperatures or precipitation during the growing season (October–May) at these four locations. The cross-wavelet power spectrum indicated that the 10-year and 22-year variations of wheat yields were mostly related to winter (December–January–February, DJF) temperature and May precipitation at all four locations, and the phase relationship for both 10-year and 22-year variations were in 'in-phase' (i.e., winter temperature or May precipitation simultaneously fluctuated with wheat yields in the same direction for 10-year and 22-year periods). For example, Fig. 6 shows the XWT between winter temperature, May precipitation, and wheat yield in N-AL. The cross-wavelet power spectrums were high for both 10-year and 22-year variations and the phase relationship for were in 'in-phase', which means low (or high) May precipitation or winter temperature is associated with low (or high) wheat yields, suggesting a strong causal relationship. Similar relationships were detected for the locations at S-AL, S-GA, and N-FL (data not shown).

3.3. XWT of crop yields and large-scale climate indices

XWT was conducted between wheat production and climate indices and between maize production and climate indices for the same four locations in the southeast USA. Again, since no decadal variations were detected for maize yields, only wheat data are

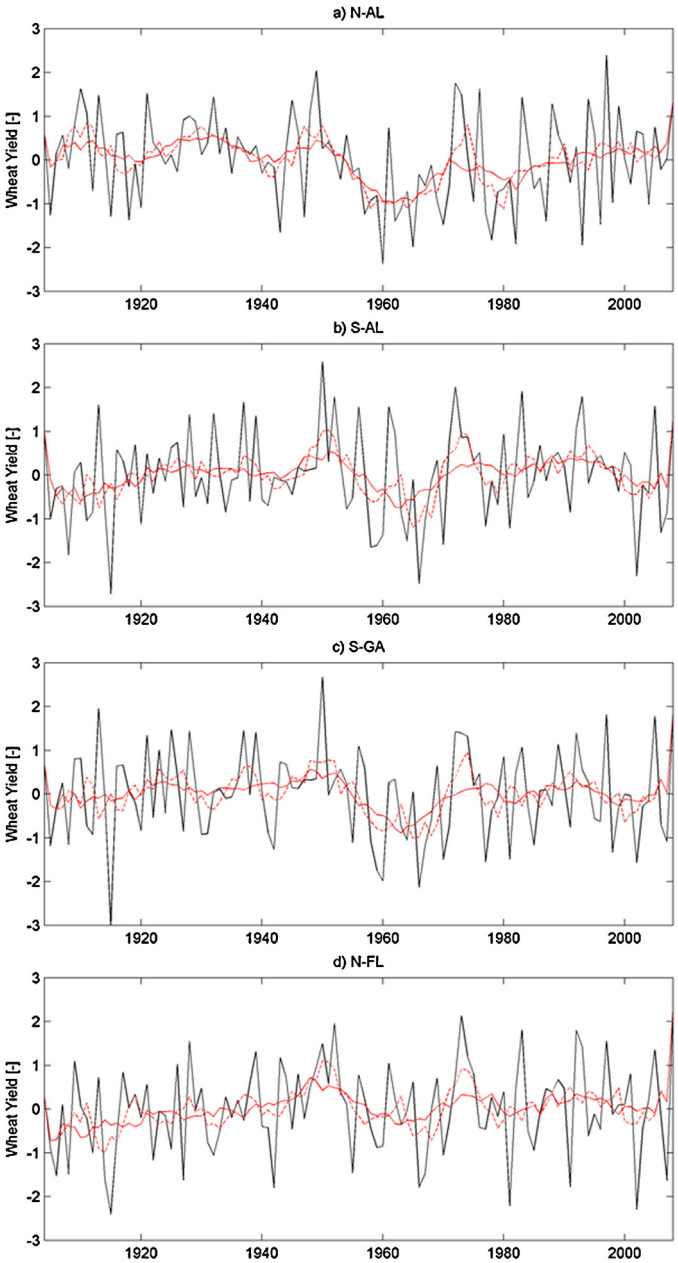

Fig. 4. Time series plot of wheat yields from 1903 to 2008 at four locations (a) N-AL, (b) S-AL, (c) S-GA, and (d) N-FL in the southeast USA. Black line, red full line, and red dotted line are original time series, 11-year moving average, and 5-year moving average, respectively.

presented. Fig. 7 shows, in N-AL, the 22-year variability appears to be correlated to all three indices (annual mean AMO index, annual mean PDO index, and winter NAO index) with the highest and statistically significant cross-wavelet power spectrum values for the annual mean PDO index, followed by winter NAO index, and annual mean AMO index.

The 10-year variability appears to be mainly driven by the NAO winter index but is also correlated with the annual mean AMO index. Note, for the 22-year variability phase relationship, while the PDO and wheat yields are in in-phase (for example, low (or high) PDO is associated with low (or high) wheat yield), the NAO and wheat yields are in opposite phase (for example, low (or high) NAO is associated with high (or low) wheat yield), which suggests that the PDO and NAO effect weaken each other. Similar XWT

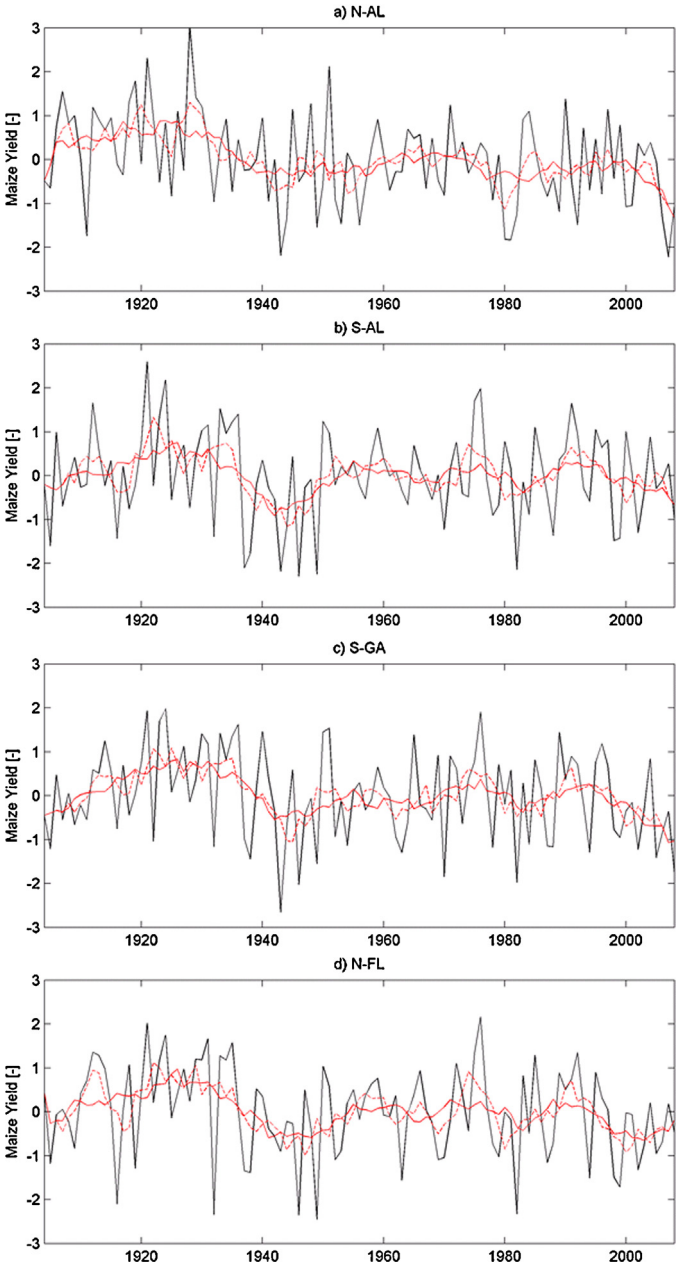

Fig. 5. As in Fig. 4, but for maize yields.

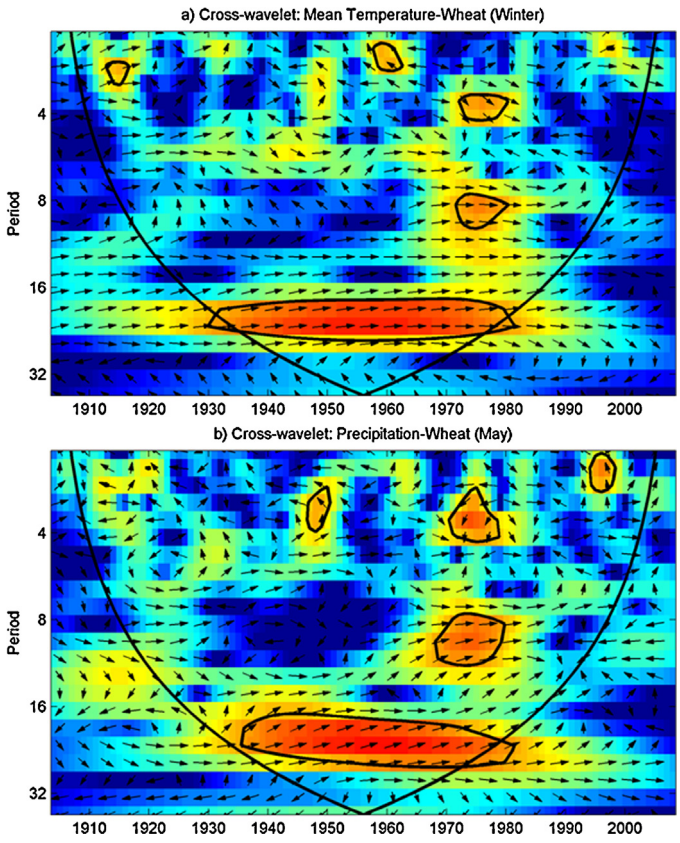

Fig. 6. Cross-wavelet power spectrum of wheat yields and (a) winter (DJF) temperature, (b) May precipitation in N-AL. The red color pixels represent highest cross-wavelet power spectrum. The black contour (surrounding red and orange areas) designates the 5% significance level against "red noise". Inside the black cone shape contour is the region without an edge effect. Outside the black cone contour is the region of cone of influence (COI) – which is due to the finite length of the time series where the edge effects become important and distort the results. The relative phase relationship is shown as arrows (with in-phase pointing right, anti-phase pointing left, and temperature or precipitation leading wheat yields by 90 degree pointing straight down)[For interpretation of the references to color in this figure legend, the reader is referred to the web version of this article].

patterns were also found for the other three locations at S-AL, S-GA, and N-FL (data not shown).

4. Discussion

In this study, we have detected short-term (e.g., a few years) and decadal variations in simulated winter crop yields (e.g., wheat) driven by climate reanalysis in the southeast USA. Furthermore, we found that there were short-term (seasonal to interannual) variations in simulated summer crop yields (e.g., maize) in the southeast USA. These decadal variations of simulated winter crop yields were associated with decadal variations in boreal winter season temperature and spring (i.e., May) precipitation. This is because winter temperature is important to vernalization of winter wheat and spring precipitation determines soil water availability to wheat growth such as stem elongation, heading, and flowering during spring season. In addition, the simulated winter wheat yields in the southeast USA showed strong correlations with decadal-time scale climate indices, including annual mean AMO index, annual mean PDO index, and the winter NAO index. There were no significant decadal variations in simulated summer crop production. This is because temperature and precipitation have no decadal climate variation during the summer growing season.

These findings are significant given the fact that seasonal climate and crop yields forecasts often have low skill and therefore, little value in crop management in many parts of the world (Ash et al., 2007; Vizard and Anderson, 2009; Wang et al., 2009; McIntosh et al., 2007; Mauget et al., 2009; Letson et al., 2009; Messina et al., 1999), including the southeastern USA (Cabrera et al., 2007; Jones et al., 2000; Stefanova et al., 2012; Tian et al., 2014). The knowledge of teleconnections between decadal climate variability and local seasonal climate variability could be potentially useful to further refining seasonal forecasts to improve seasonal crop management. For example, knowing the phase of the AMO, PDO, and NAO will provide further information of the influence of seasonally forecasted ENSO teleconnection on a winter crop like wheat in the southeast USA. The AMO and PDO have a broad temporal variability in the time range of 50–70 years and 20–30 years, respectively. The NAO on the other hand has far broader temporal variability with periods ranging from a few years to decades apart. These oscillations have shown some degrees of predictability in current dynamic climate models (e.g., Johansson, 2007; Wen

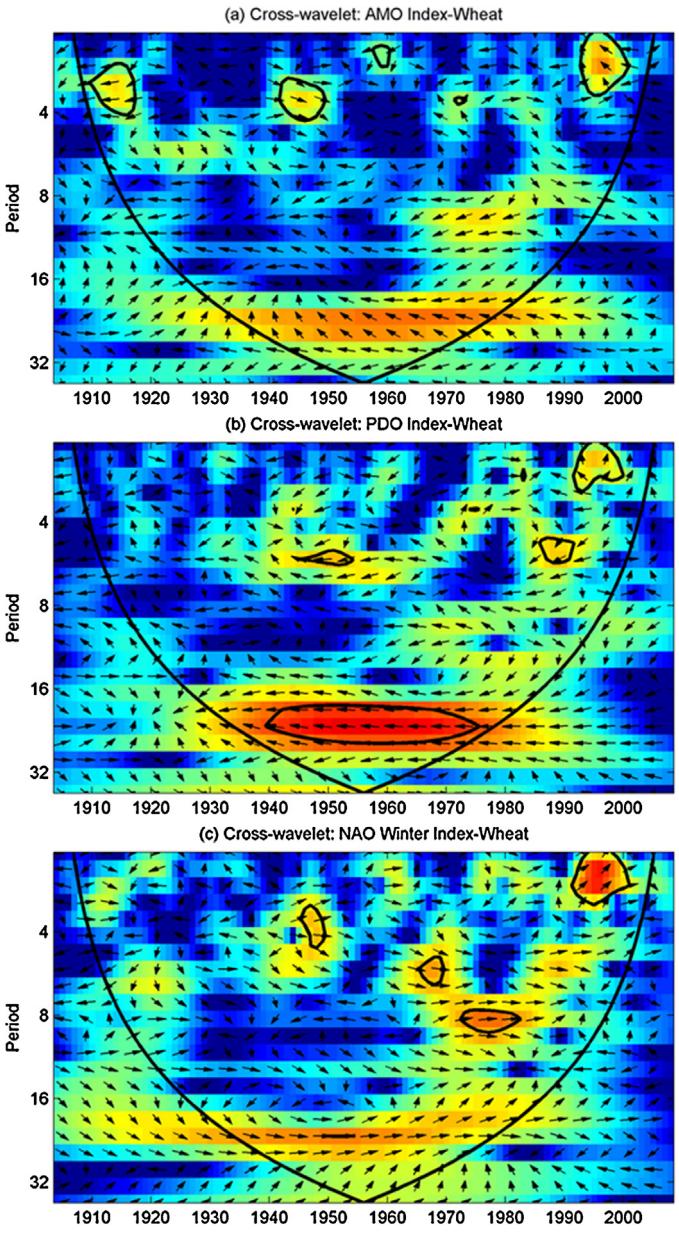

Fig. 7. Cross-wavelet power spectrum of wheat yields and (a) annual mean AMO, (b) annual mean PDO, and (c) winter NAO for N-AL. The red color pixels represent highest cross-wavelet power spectrum. The black contour (surrounding red and orange areas) designates the 5% significance level against "red noise". Inside the black cone shape contour is the region without an edge effect. Outside the black cone contour is the region of cone of influence (COI) – which is due to the finite length of the time series where the edge effects become important and distort the results. The relative phase relationship is shown as arrows (with in-phase pointing right, anti-phase pointing left, and the climate index leading wheat yields by 90 degree pointing straight down)[For interpretation of the references to color in this figure legend, the reader is referred to the web version of this article].

et al., 2012; Yang et al., 2013). In addition, the inertia of their low frequency variations offer an opportunity to exploit their forcing on higher frequency variability. Several decadal reforecasts conducted as part of the IPCC AR5 have demonstrated that climate models can derive skill from the persistence, for example, of the AMO in the initial condition for a decade (Corti et al., 2012; Doblas-Reyes et al., 2011). From the application point of view, empirical models can be developed using these observed large-scale climate information to improve seasonal crop management. Seasonal prediction of these climate oscillations from dynamic climate models can be used or combined with empirical- or process-based crop models to assist crop management. The effects of long-term climate patterns such as the AMO, PDO, and NAO are not just limited to a particular region. Besides the southeast USA, the importance of these long-term climate patterns for crop productions were also found in other regions of the world (e.g., Atkinson et al., 2005; Gimeno et al., 2002; Persson et al., 2012). Similar to ENSO impacts on crop yields at a global scale (Iizumi et al., 2014), long-term climate patterns such as the AMO, PDO, and NAO could also be considered when investigating the climate impacts on global crop production.

This study provides quantitative information that is essential to investigate the effects of climate change on crop production. For example, since climate-driven simulated winter crop production showed strong decadal variations in a region, the decadal variability should be separated from climate change signals when investigating the agricultural effects from climate change.

Dynamically downscaled reanalysis was used to drive CSMs to simulate crop production by keeping other factors constant, so that the climate variability effects on crop production could be separated. However, the reanalysis-driven crop simulations have uncertainties from different sources such as the reanalysis data and the CSM (Asseng et al., 2013; Cammarano et al., 2013). The atmospheric reanalysis data (FLAReS1.0) used in this study is an atmospheric model dependent product, which is influenced and limited by the fidelity of the atmospheric model. Similarly the CSM is a numerical, discretized representation of crop growth and development which also has limitations (Asseng et al., 2013). Furthermore, this study only considered one soil type and different soil types might also impact on the soil-climate interactions and consequently the yield-climate correlations.

5. Conclusion

A wavelet analysis revealed that there were strong decadal variations for simulated winter crop yields but not for simulated summer crop yields in the southeast USA. Simulated winter crop yields were dominated by 10- and 22-years decadal oscillations, which are associated with decadal variations in winter temperature and May precipitation. Simulated winter wheat yields were positively or negatively correlated with the AMO, PDO, and NAO winter indices for decadal periods. No decadal variations were detected for simulated summer crop production. This knowledge of decadal variability could be potentially useful to refine seasonal forecasting of crop management.

Acknowledgments

This research was supported by NOAA-OAR-CPO-2010-2001720 RISA funding for the Southeast Climate Consortium (SECC). The software package for performing CWT and XWT is available at: http://noc.ac.uk/using-science/crosswavelet-wavelet-coherence. The authors thank Dr. Kenneth J. Boote of the University of Florida for his useful discussions. The authors thank three anonymous reviewers for their useful comments.

References

Ash, A., McIntosh, P., Cullen, B., Carberry, P., Smith, M.S., 2007. Constraints and opportunities in applying seasonal climate forecasts in agriculture. Aust. J. Agric. Res. 58 (10), 952–965.
Asseng, S., 2004. Wheat Crop Systems: A Simulation Analysis. CSIRO Publishing.
Asseng, S., et al., 2013. Uncertainty in simulating wheat yields under climate change. Nat. Clim. Change 3 (9), 827–832.
Asseng, S., McIntosh, P.C., Wang, G., Khimashia, N., 2012a. Optimal N fertiliser management based on a seasonal forecast. Eur. J. Agron. 38 (0), 66–73.
Asseng, S., Thomas, D., McIntosh, P., Alves, O., Khimashia, N., 2012b. Managing mixed wheat–sheep farms with a seasonal forecast. Agric. Syst. 113, 50–56.
Atkinson, M.D., Kettlewell, P.S., Hollins, P.D., Stephenson, D.B., Hardwick, N.V., 2005. Summer climate mediates UK wheat quality response to winter North Atlantic Oscillation. Agric. For. Meteorol. 130 (1), 27–37.

Baigorria, G.A., et al., 2010. Forecasting cotton yield in the Southeastern United States using coupled global circulation models. J. Agron. 102 (1), 187–196.
Baigorria, G.A., Hansen, J.W., Ward, N., Jones, J.W., O'Brien, J.J., 2008a. Assessing predictability of cotton yields in the Southeastern United States based on regional atmospheric circulation and surface temperatures. J. Appl. Meteor. Climatol. 47 (1), 76–91.
Baigorria, G.A., Jones, J.W., O'Brien, J.J., 2008b. Potential predictability of crop yield using an ensemble climate forecast by a regional circulation model. Agric. For. Meteorol. 148 (8–9), 1353–1361.
Bannayan, M., Sanjani, S., Alizadeh, A., Lotfabadi, S.S., Mohamadian, A., 2010. Association between climate indices, aridity index, and rainfed crop yield in Northeast of Iran. Field Crop Res. 118 (2), 105–114.
Brown, I., 2013. Influence of seasonal weather and climate variability on crop yields in Scotland. Int. J. Biometeorol. 57 (4), 605–614.
Cabrera, V.E., Letson, D., Podesta, G., 2007. The value of climate information when farm programs matter. Agric. Syst. 93 (1–3), 25–42.
Cammarano, D., et al., 2013. Evaluating the fidelity of downscaled climate data on simulated wheat and maize production in the Southeastern US. Reg. Environ. Change 13 (1), 101–110.
Cantelaube, P., Terres, J.-M., 2005. Seasonal weather forecasts for crop yield modelling in Europe. Tellus A 57 (3), 476–487.
Carey, S.K., Tetzlaff, D., Buttle, J., Laudon, H., McDonnell, J., McGuire, K., Seibert, J., Soulsby, C., Shanley, J., 2013. Use of color maps and wavelet coherence to discern seasonal and interannual climate influences on streamflow variability in northern catchments. Water Resource Res. 49, 6194–6207, http://dx.doi.org/10.1002/wrcr.20469.
Challinor, A.J., Wheeler, T.R., Slingo, J.M., Craufurd, P.Q., Grimes, D.I.F., 2005. Simulation of crop yields using ERA-40: limits to skill and nonstationarity in weather – yield relationships. J. Appl. Meteorol. 44 (4), 516–531.
Corti, S., Weisheimer, A., Palmer, T.N., Doblas-Reyes, F.J., Magnusson, L., 2012. Reliability of decadal predictions. Geophys. Res. Lett. 39, L21712, http://dx.doi.org/10.1029/2012G L0 53354.
Compo, G.P., et al., 2011. The Twentieth Century Reanalysis Project. Q. J. R. Meteorol. Soc. 137 (654), 1–28.
Coulibaly, P., Burn, D.H., 2004. Wavelet analysis of variability in annual Canadian streamflows. Water Resour. Res. 40, http://dx.doi.org/10.1029/2003WR002667, W03105.
DiNapoli, S.M., Misra, V., 2012. Reconstructing the 20th century high-resolution climate of the southeastern United States. J. Geophys. Res.: Atmos. 117 (D19), D19113.
Doblas-Reyes, F.J., Balmaseda, M.A., Palmer, T.N., 2011. Decadal climate prediction with the ECMWF coupled forecast system: impact of ocean observations. J. Geophys. Res. 116, http://dx.doi.org/10.1029/2010KD015394, D19111.
Enfield, D.B., Mestas-Nuñez, A.M., Trimble, P.J., 2001. The Atlantic Multidecadal Oscillation and its relation to rainfall and river flows in the continental U.S. Geophys. Res. Lett. 28 (10), 2077–2080.
Gimeno, L., Ribera, P., Iglesias, R., de la Torre, L., García, R., Hernández, E., 2002. Identification of empirical relationships between indices of ENSO and NAO and agricultural yields in Spain. Clim. Res. 21 (2), 165–173.
Grinsted, A., Moore, J.C., Jevrejeva, S., 2004. Application of the cross wavelet transform and wavelet coherence to geophysical time series. Nonlinear Process. Geophys. 11 (5/6), 561–566.
Hansen, J.W., Hodges, A.W., Jones, J.W., 1998. ENSO Influences on agriculture in the Southeastern United States. J. Clim. 11 (3), 404–411.
Hansen, J.W., Jones, J.W., Kiker, C.F., Hodges, A.W., 1999. El Niño – Southern Oscillation impacts on winter vegetable production in Florida. J. Clim. 12 (1), 92–102.
Hoogenboom, G., 2000. Contribution of agrometeorology to the simulation of crop production and its applications. Agric. For. Meteorol. 103 (1–2), 137–157.
Hoogenboom, G., Jones, J.W., Wilkens, P.W., Porter, C.H., Boote, K.J., Hunt, L.A., Singh, U., Lizaso, J.L., White, J.W., Uryasev, O., Royce, F.S., Ogoshi, R., Gijsman, A.J., Tsuji, G.Y., Koo, J., 2010. Decision Support System for Agrotechnology Transfer (DSSAT) Version 4.5 [CD-ROM]. University of Hawaii, Honolulu Hawaii.
In: Hurrell, J., National Center for Atmospheric Research Staff (Eds.). Last modified 20 June 2014. The Climate Data Guide: Hurrell North Atlantic Oscillation (NAO) Index (station-based). Retrieved from: https://climatedataguide.ucar.edu/climate-data/hurrell-north-atlantic-oscillation-nao-index-station-based
Iizumi, T., Luo, J., Challinor, A.J., Sakurai, G., Yokozawa, M., Sakuma, H., Brown, M.E., Yamagata, T., 2014. Impacts of El Niño Southern Oscillation on the global yields of major crops. Nat. Commun., 5.
Jarlan, L., Abaoui, J., Duchemin, B., Ouldbba, A., Tourre, Y.M., Khabba, S., Page, M.L., Balaghi, R., Mokssit, A., Chehbouni, G., 2013. Linkages between common wheat yields and climate in Morocco (1982–2008). Int. J. Biometeorol., 1–14.
Johansson, A., 2007. Prediction skill of the NAO and PNA from daily to seasonal time scales. J. Clim. 20, 1957–1975.
Jones, C.A., Kiniry, J.R., Dyke, P., 1986. Ceres-maize: a Simulation Model of Maize Growth and Development, first ed. Texas A&M University Press.
Jones, J.W., Hansen, J.W., Royce, F.S., Messina, C.D., 2000. Potential benefits of climate forecasting to agriculture. Agric. Ecosyst. Environ. 82 (1–3), 169–184.
Jones, J.W., Hoogenboom, G., Porter, C.H., Boote, K.J., Batchelor, W.D., Hunt, L.A., Wilkens, P.W., Singh, U., Gijsman, A.J., Ritchie, J.T., 2003. DSSAT cropping system model. Eur. J. Agron. 18, 235–265.
Liang, S., Ge, S., Wan, L., Zhang, J., 2010. Can climate change cause the Yellow River to dry up? Water Resource Res. 46 (2).
Letson, D., et al., 2009. Value of perfect ENSO phase predictions for agriculture: evaluating the impact of land tenure and decision objectives. Clim. Change 97 (1–2), 145–170.
Mantua, N.J., Hare, S.R., Zhang, Y., Wallace, J.M., Francis, R.C., 1997. A Pacific interdecadal climate oscillation with impacts on salmon production. Bull. Am. Meteorol. Soc. 78 (6), 1069–1079.
Martinez, C.J., Baigorria, G.A., Jones, J.W., 2009. Use of climate indices to predict corn yields in southeast USA. Int. Clim. 29 (11), 1680–1691.
Martinez, C.J., Jones, J.W., 2011. Atlantic and Pacific sea surface temperatures and corn yields in the southeastern USA: lagged relationships and forecast model development. Int. J. Clim. 31 (4), 592–604.
Mauget, S., Zhang, J., Ko, J.H., 2009. The value of ENSO forecast information to dual-purpose winter wheat production in the US Southern high plains. J. Appl. Meteor. Climatol. 48 (10), 2100–2117.
Maxwell, J.T., Knapp, P.A., Ortegren, J.T., 2013. Influence of the Atlantic Multidecadal Oscillation on tupelo honey production from AD 1800 to 2010. Agric. For. Meteorol. 174, 129–134.
McCabe, G.J., Palecki, M.A., Betancourt, J.L., 2004. Pacific and Atlantic Ocean influences on multidecadal drought frequency in the United States. Proc. Natl. Acad. Sci. U. S. A. 101 (12), 4136–4141.
McIntosh, P.C., Pook, M.J., Risbey, J.S., Lisson, S.N., Rebbeck, M., 2007. Seasonal climate forecasts for agriculture: toward better understanding and value. Field Crop. Res. 104 (1–3), 130–138.
Messina, C.D., Hansen, J.W., Hall, A.J., 1999. Land allocation conditioned on El Niño-Southern Oscillation phases in the Pampas of Argentina. Agric. Syst. 60, 197–212.
Misra, V., DiNapoli, S.M., Bastola, S., 2013. Dynamic downscaling of the twentieth-century reanalysis over the southeastern United States. Reg. Environ. Change 13 (1), 15–23.
Persson, T., Bergjord, A.K., Höglind, M., Persson, T., Bergjord, A.K., Höglind, M., 2012. Simulating the effect of the North Atlantic Oscillation on frost injury in winter wheat. Clim. Res. 53 (2012), 4353.
Royce, F.S., Fraisse, C.W., Baigorria, G.A., 2011. ENSO classification indices and summer crop yields in the Southeastern USA. Agric. For. Meteorol. 151 (7), 817–826.
Seager, R., Kushnir, Y., Nakamura, J., Ting, M., Naik, N., 2010. Northern Hemisphere winter snow anomalies: ENSO, NAO and the winter of 2009/10. Geophys. Res. Lett. 37 (14), L14703.
Stefanova, L., Misra, V., O'Brien, J.J., Chassignet, E.P., Hameed, S., 2012. Hindcast skill and predictability for precipitation and two-meter air temperature anomalies in global circulation models over the Southeast United States. Clim. Dyn. 38 (1–2), 161–173.
Tian, D., Martinez, C.J., Graham, W.D., Hwang, S., 2014. Statistical downscaling multi-model forecasts for seasonal precipitation and surface temperature over southeastern USA. J. Clim. 27, 8384–8411.
Torrence, C., Compo, G.P., 1998. A practical guide to wavelet analysis. Bull. Am. Meteorol. Soc. 79 (1), 61–78.
van Ittersum, M.K., et al., 2003. On approaches and applications of the Wageningen crop models. Eur. J. Agron. 18 (3–4), 201–234.
Vizard, A.L., Anderson, G.A., 2009. The resolution and potential value of Australian seasonal rainfall forecasts based on the five phases of the Southern Oscillation index. Crop Pasture Sci. 60 (3), 230–239.
Wang, E.L., McIntosh, P., Jiang, Q., Xu, J., 2009. Quantifying the value of historical climate knowledge and climate forecasts using agricultural systems modelling. Clim. Change 96 (1–2), 45–61.
Wen, C., Xue, Y., Kumar, A., 2012. Seasonal prediction of North Pacific SSTs and PDO in the NCEP CFS Hindcasts. J. Clim. 25, 5689–5710.
Yang, X., et al., 2013. A predictable AMO-like pattern in the GFDL fully coupled ensemble initialization and decadal forecasting system. J. Clim. 26, 650–661.